Available online at www.sciencedirect.com

SciVerse ScienceDirect

Scripta Materialia 66 (2012) 1–4

Scripta MATERIALIA

www.elsevier.com/locate/scriptamat

Three-dimensional grain structure of sintered bulk strontium titanate from X-ray diffraction contrast tomography

M. Syha,[a,*] W. Rheinheimer,[a] M. Bäurer,[a] E.M. Lauridsen,[b] W. Ludwig,[c] D. Weygand[a] and P. Gumbsch[a,d]

[a] *Karlsruhe Institute for Technology, Institute for Applied Materials, Kaiserstr. 12, 76128 Karlsruhe, Germany*
[b] *Risø National Laboratory, Fredrigsborgvej 399, 4000 Roskilde, Denmark*
[c] *European Synchrotron Radiation Facility, 6 Rue Jules Horowitz, 38043 Grenoble, France*
[d] *Fraunhofer Institut für Werkstoffmechanik, Wöhlerstr. 11, 79108 Freiburg, Germany*

Received 17 June 2011; revised 5 August 2011; accepted 8 August 2011
Available online 26 August 2011

The three-dimensional grain boundary network of sintered bulk strontium titanate is reconstructed using X-ray diffraction contrast tomography, a non-destructive technique for determining the grain shape and crystallographic orientation in polycrystals that is ideally suited for detailed studies of microstructure evolution. We present the first microstructure reconstruction of a perovskite comprising 849 grains and detailed interface orientation evaluations of individual grains. Comparison of structural and topological quantities to metallographic investigations and statistical grain models demonstrates the method's validity and applicability.

Keywords: 3-D reconstruction; Microstructure; X-ray diffraction; Perovskite; 3-D tomography

The macroscopic material properties of polycrystalline materials are strongly determined by the crystallographic orientation, morphology and size of individual grains. Hence a proper microstructure characterization is of great importance, especially for highly anisotropic materials, such as most perovskites [1,2]. Unfortunately, little is known about the relationship between microstructure evolution and interface anisotropies in these materials. The present investigations were performed on strontium titanate ($SrTiO_3$), which is a well-established model system for perovskite ceramics due to its stable cubic structure in the investigated temperature range. Several experimental investigations indicate a highly orientation and temperature dependent interface energy for strontium titanate [1,3]. Moreover, the growth kinetics of strontium titanate shows an unusual deviation from the expected Arrhenius behaviour [4] which is not yet well understood and requires further investigation in terms of well-controlled annealing experiments. In order to study correlations between grain boundary properties and microstructure evolution, and to allow for modelling of this behaviour, truly three-dimensional (3-D) microstructural information needs to be acquired at various stages during grain growth [5].

The bulk material for the X-ray diffraction contrast tomography (DCT) specimen was prepared from $SrTiO_3$ powders processed by the mixed oxide route from $SrCO_3$ and TiO_2 (both 99.9+%, Sigma Aldrich Chemie, Taufkirchen, Germany) using a molar Sr/Ti ratio of 0.996. The powder was milled, calcined (6 h at 975 °C) and subsequently milled again. The specimens were uniaxially pressed to a cylindrical shape and isostatically pressed to increase the green density. Finally, the specimens were sintered at 1600 °C in an oxygen atmosphere yielding a material with an average grain radius of 14.1 ± 1.5 μm. Further details on the fabrication process and extensive microstructure investigations of the material are provided in Refs. [4,6]. Cylindrical samples were then prepared for the X-ray investigations. The material was therefore cut into small discs (3 mm in diameter and 1 mm in thickness) which were then ground to a diameter of approximately 300 μm using a turning lathe and abrasive paper.

X-ray DCT [7] is a unique non-destructive method that allows reconstruction of the 3-D grain shape and crystallographic orientation of micrometer-scale grains in polycrystalline bulk materials. The experiment was performed

* Corresponding author. E-mail: melanie.syha@kit.edu

1359-6462/$ - see front matter © 2011 Acta Materialia Inc. Published by Elsevier Ltd. All rights reserved.
doi:10.1016/j.scriptamat.2011.08.005

at the materials science beamline ID11 of the European Synchrotron Radiation Facility (ESRF), Grenoble, France. The principles of DCT and the subsequent data analysis are described in detail in Refs. [7–9]. The dedicated tomographic set-up for our experiment consists of a rotating sample-holder combined with a high-resolution 2-D detection system with a pixel size of 1.4 μm. The experiment was carried out with a beam energy of 36 keV and a sample–detector distance of 3.23 mm. A monochromatic X-ray beam illuminates both the sample and the detector. Extinction as well as diffraction information was recorded in 0.05° increments during 360° scans, allowing for Friedel pair recognition. Naturally, a grain fulfils the Bragg condition for diffraction up to four times in such a full rotation scan, providing an ample number of diffraction and extinction spots per grain. A crystallographic indexing scheme as described in Ref. [9] was adapted to perovskite materials with space group 225 and applied to this dataset. The shape and position reconstruction itself was done by means of algebraic reconstruction techniques (ARTs) [10]. The subsequent post-processing step combines a uniform morphological dilation procedure which renders the grain structure volume filling [8] with the subtraction of the collective pore volume which was gathered separately using phase-contrast imaging techniques [11]. Phase-contrast data was acquired with a pixel size of 0.56 μm yielding high-resolution images in a comparatively short scanning time (phase-contrast scans were done in 0.72° increments).

A first 3-D reconstruction of a cylindric strontium titanate specimen investigated by 3-D X-ray DCT is shown in Figure 1a. The comparison of a cross-section through the reconstructed specimen (Fig. 1b) and a scanning electron microscopy (SEM) micrograph (Fig. 1c) taken from the bulk material shows that similar and realistic grain shapes are identified.

The black areas in Figure 1b indicate the location of pores. Due to the fact that the porosity is obtained by means of phase-contrast imaging, pores with a volume of several voxels can be detected with high accuracy. The relative porosity of the reconstructed microstructure (2.6 ± 0.1 vol.%) is in excellent agreement with the porosity data measured directly from the sample material (3.0 ± 0.4 vol.%). The spatial arrangement of the pores is shown in Figure 1d.

The sample contains a total of 849 grains, of which 434 are connected with one of the surfaces and 415 are completely surrounded by other grains and are therefore termed bulk grains. The grain size distribution for the sample and for the subset of bulk grains can be fitted with log-normal distributions (Fig. 2). The average grain radius $\langle r \rangle$ evaluated from the bulk grain volume (the values including surface grains are given in parentheses) approximated as a sphere is 14.3 μm (14.7 μm) and the fitted log-normal distribution has a standard deviation of $\sigma = 0.47$ ($\sigma = 0.52$).

Measurements of the equivalent circle diameter (ECD) on cross-sections of the reconstructed structure reveal an average grain radius $\langle r \rangle$ of 13.0 μm. The corresponding value obtained by measuring ECD on conventional 2-D micrographs obtained by SEM was found to be 14.1 μm. A comparison of the 2-D distributions evaluated from DCT and SEM is given in Figure 2. Although all three distributions can be fitted as log-normal distributions, this fit holds best for the distribution obtained from 3-D DCT data. The goodness of fit, measured as chi square, is 27 for 3-D DCT data, 97 for 2-D DCT data and 127 for the distribution obtained from the micrographs.

The average number of faces per grain was found to be $\langle F_G \rangle = 12.8 \pm 0.1$ considering only bulk grains and $\langle F_G \rangle = 12.1 \pm 0.2$ considering all grains. Both values include interfaces between grains and pores. Obviously,

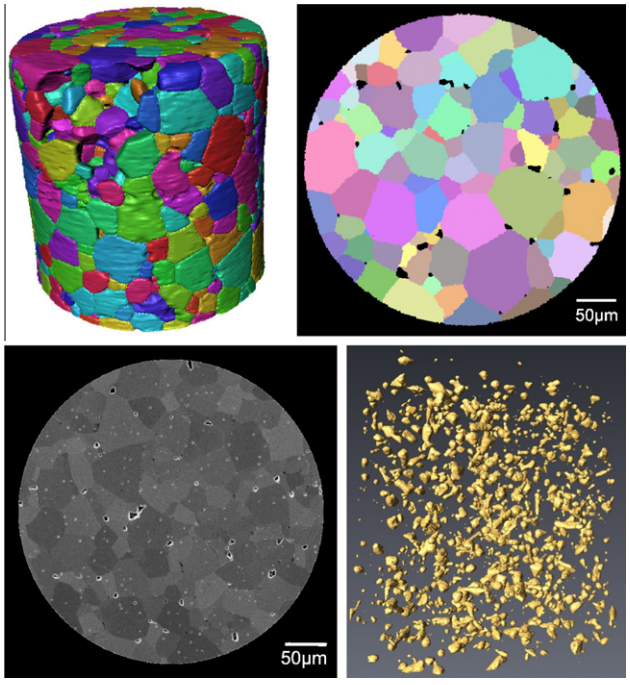

Figure 1. 3-D view (a) (colored randomly) and cross-section (colored according to crystallographic orientation) (b) of the reconstructed structure compared to a SEM micrograph (c) of the same material. Collective ensemble of intergranular pores (d).

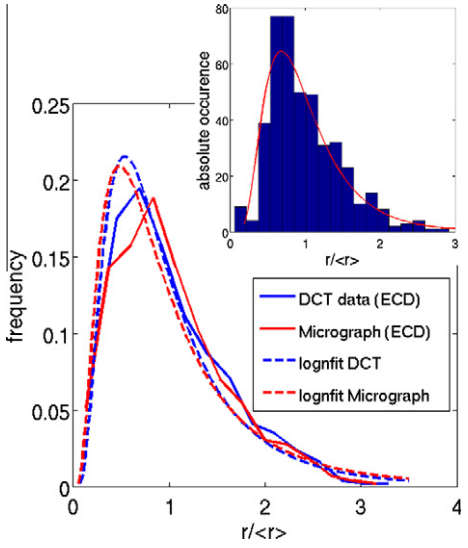

Figure 2. Comparison of grain size distributions obtained by equivalent circle diameter measurements on bulk DCT data and conventional micrographs. (Inset) Grain size distribution of bulk grains derived from grain volumes.

the first value is more relevant since outer grains consist naturally of a reduced number of faces due to their contribution to the sample surface. The average number of edges per grain is found to be $\langle E_G \rangle = 32.2 \pm 0.8$ with an average number of $\langle E_F \rangle = 4.9 \pm 0.1$ edges per grain face for the bulk material.

The grain boundary misorientation distribution resembles a perfect Mackenzie plot, indicating a texture-free material. Initial investigations of local grain boundary orientations, however, reveal some preference for $\langle 100 \rangle$ interface normals with respect to the crystallographic orientation of the considered grain. Figure 3 shows a reconstructed bulk grain where the grain boundary triangulation is colored according to the local interface normal orientation. Although this grain consists of 55 faces, its overall shape deviates significantly from a sphere and can rather be described as cube with truncated edges showing a clear preference for $\langle 100 \rangle$ interface normals.

The results show that the X-ray DCT technique is very well suited for the microstructure reconstruction of perovskite materials. The grain shape is visually identical to conventional 2-D micrographs and the resolution at the grain boundaries is of reasonable quality.

Since our ceramic material is free of dislocations, second-phase particles and orientation or strain gradients, we expect to have the same or better orientation space resolution as obtained in investigations on recrystallized aluminum 1050 alloy [8] using a similar experimental set-up. There, the achievable accuracy for the resolution of the crystallographic orientation was estimated to be below 0.1°. The resolution of the crystallographic orientation of individual interface planes is of course affected by the uniform dilation procedure. On average, a radial dilation of 2.63 μm per grain is applied in order to achieve a dense material. The orientation of the interface normal of a grain boundary with an average length of $\langle r \rangle = 14.3$ μm can therefore be given approximately within ±10°. However, visual inspection of the location and shape of the pores reveals that more than 80% of the pores are located at triple lines. These pores are consistently connected to the outgoing grain boundaries (see Fig. 1c). Therefore, we conclude that the true interface normal uncertainty is significantly below the ±10° given above.

The good agreement between the grain size distributions obtained from DCT and SEM underline the plausibility of the reconstruction. The average grain radius is of the expected size and the difference in the average grain radius obtained over all grains and bulk grains only is below the resolution. While at first sight one would possibly have expected a smaller average grain radius for the truncated outer grains, this is not significant in terms of the current data, since larger grains are also preferentially cut and consequently a larger fraction of smaller grains is embedded in the bulk material. The average bulk grain radius may therefore be slightly underestimated.

The average number of faces per grain $\langle F_G \rangle = 12.8$ and edges per grain face $\langle E_F \rangle = 4.9$ are quite close to statistical grain models such as Coxeter's space-filling polytopes [12] ($\langle F_G \rangle = 13.7$, $\langle E_F \rangle = 5.1$), Kelvin's α-tetrakaidecahedrons or Williams' β-tetrakaidecahedrons (both $\langle F_G \rangle = 14$, $\langle E_F \rangle = 5.1$) [13,14], which all assume isotropic growth conditions. Small numbers of faces per grain have also been reported for other anisotropic polycrystals [15,16]. We therefore assume that this topological quantity may be affected by interface anisotropy. This effect is currently under investigation using 3-D grain growth simulations [17].

As expected for an undeformed polycrystal obtained by sintering, the misorientation distribution follows a perfect Mackenzie plot Figure 4. However, the interface orientations clearly display the existence of preferred grain boundary orientations. The reconstructed microstructure reveals that grains with a global outer shape close to a $\langle 100 \rangle$-oriented cube were present as shown in Figure 3. This is in excellent agreement with capillarity vector reconstruction results that show an energy minimum for $\{100\}$ interfaces [1].

Each side of the cube-shaped grain is composed of several grain boundaries, oriented along $\langle 001 \rangle$ directions with respect to the grain reference frame. This clearly demonstrates that an energetically favorable orientation with respect to one crystallite is sufficient in

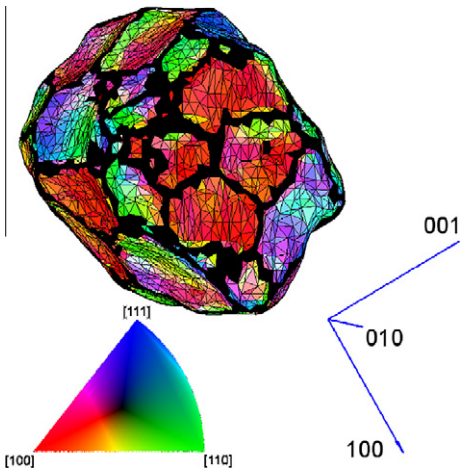

Figure 3. Single bulk grain colored according to the local interface normal orientation after surface triangulation. The grain shows several rather flat faces with $\langle 100 \rangle$ surface normals.

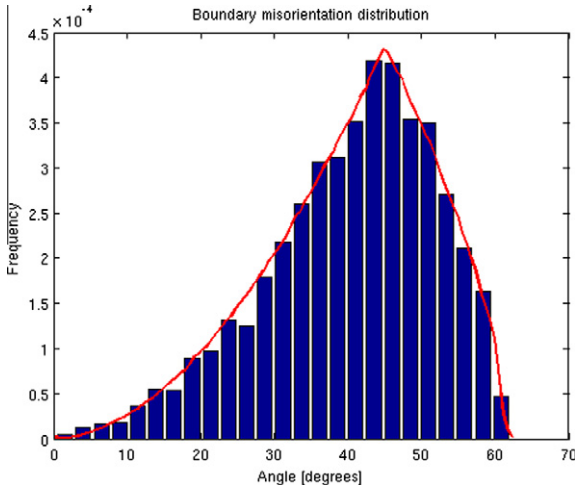

Figure 4. The relative frequency of the misorientations between neighboring grains shown as blue bars is in good agreement with the solid red line marking the Mackenzie distribution.

strontium titanate to affect the global interface orientation and thus the grain morphology severely. A similar behaviour has already been observed for grain boundaries surrounding abnormally growing grains in strontium titanate [18]. There, too, the general interface orientation is parallel to the ⟨100⟩ orientations of the abnormally growing grain. These transmission electron microscopy observations indicate that the grain boundaries are curved close to triple lines; boundary segments away from these triple lines can be atomically flat on the micrometer scale [19,18]. In the current study no abnormal grains were present.

The acquired crystallography data allows for a detailed analysis of the microstructure of ceramic materials composed of the 3-D grain boundary network and the 3-D distribution of pores. It gives both misorientation and inclination distributions that can be correlated to the morphology. This information is certainly of practical use for the analysis of sintering processes but also provides an ideal basis for the comparison to grain growth simulations.

It is straightforward to extend these investigations to repeated DCT analysis of the same sample during interrupted or in situ annealing experiments. This will not only help to understand the densification during sintering but also give access to the time evolution of an evolving grain boundary network. Combined with grain growth simulations, this can be used to directly obtain the grain boundary mobility data that is needed to calibrate mesoscale grain growth models [20,17].

This work was supported by the Deutsche Forschungsgemeinschaft (DFG) under Contract WE3544/4-1 and BA4143/2-1. We kindly acknowledge the Karlsruhe House of Young Scientists (KHYS) for covering travel expenses of one of the authors (M.S.), the European Synchrotron Radiation Facility (ESRF) for provision of beam time and Loredana Erra, beam line ID11, for technical support.

[1] T. Sano, D. Saylor, G. Rohrer, Journal of the American Ceramic Society 86 (2003) 1933–1939.
[2] B. Lee, S. Chung, S. Kang, Acta Materialia 48 (2000) 1575–1580.
[3] S. Lee, W. Sigle, W. Kurtz, M. Rühle, Acta Materialia 51 (2003) 975–981.
[4] M. Bäurer, D. Weygand, P. Gumbsch, M. Hoffmann, Scripta Materialia 61 (2009) 584–587.
[5] M. Syha, M. Bäurer, M. Hoffmann, E. Lauridsen, W. Ludwig, D.Weygand, P. Gumbsch, Proceedings of the 31st Risø International Symposium on Materials Science (2010) 138–140.
[6] M. Bäurer, H. Kungl, M. Hoffmann, Journal of the American Ceramic Society 92 (2009) 601–606.
[7] W. Ludwig, S. Schmidt, E. Lauridsen, H. Poulsen, Journal of Applied Crystallography 41 (2008) 302–309.
[8] G. Johnson, A. King, M. Honnicke, J. Marrow, W. Ludwig, Journal of Applied Crystallography 41 (2008) 310–318.
[9] W. Ludwig, P. Reischig, A. King, M. Herbig, E. Lauridsen, G. Johnson, T. Marrow, J. Buffière, Review of Scientific Instruments (2009) 033905.
[10] A. Kak, M. Slaney, Principles of Computerized Tomographic Imaging, IEEE Press, 1987.
[11] P. Cloetens, M. Pateyron-Salomé, J.Y. Buffière, G. Peix, J. Baruchel, F. Peyrin, M. Schlenker, Journal of Applied Physics 81 (1997) 5878.
[12] H. Coxeter, Illinois Journal of Mathematics 2 (1958) 746–758.
[13] C. Smith, Metallurgical Reviews 9 (1964) 1–48.
[14] R. Williams, Science 161 (1968) 266–267.
[15] F. Hull, Material Science and Technology 4 (1988) 778–785.
[16] W. Williams, C. Smith, Transactions on AIME 194 (1952) 755.
[17] M. Syha, D. Weygand, Modelling and Simulation in Materials Science and Engineering 18 (2010) 015010.
[18] S. Shih, S. Lozano-Perez, D. Cockayne, Journal of Materials Research 25 (2010) 260–265.
[19] M. Bäurer, H. Störmer, D. Gerthsen, M. Hoffmann, Advanced Engineering Materials 12 (2010) 1230–1234.
[20] D. Weygand, Y. Bréchet, J. Lépinoux, W. Gust, Philosophical Magazine B 79 (1999) 703–716.